Identification of S-phase DNA damage-response targets in fission yeast reveals conservation of damage-response networks

Identification of S-phase DNA damage-response targets in fission yeast reveals conservation of damage-response networks

Nicholas A. Willis[a,1,2], Chunshui Zhou[b,c,2], Andrew E. H. Elia[b,d], Johanne M. Murray[e], Antony M. Carr[e], Stephen J. Elledge[b,f,3], and Nicholas Rhind[a,3]

[a]Department of Biochemistry and Molecular Pharmacology, University of Massachusetts Medical School, Worcester, MA 01605; [b]Department of Genetics, Division of Genetics, Brigham and Women's Hospital, Harvard Medical School, Boston, MA 02115; [c]The Laboratory of Medical Genetics, Harbin Medical University, Harbin, China, 150081; [d]Department of Radiation Oncology, Massachusetts General Hospital, Boston, MA 02114; [e]Genome Damage and Stability Centre, School of Life Sciences, University of Sussex, Falmer, BN1 9RQ, United Kingdom; and [f]Howard Hughes Medical Institute, Harvard Medical School, Boston, MA 02115

Contributed by Stephen J. Elledge, February 16, 2016 (sent for review December 28, 2015; reviewed by Mingxia Huang and Lee Zou)

The cellular response to DNA damage during S-phase regulates a complicated network of processes, including cell-cycle progression, gene expression, DNA replication kinetics, and DNA repair. In fission yeast, this S-phase DNA damage response (DDR) is coordinated by two protein kinases: Rad3, the ortholog of mammalian ATR, and Cds1, the ortholog of mammalian Chk2. Although several critical downstream targets of Rad3 and Cds1 have been identified, most of their presumed targets are unknown, including the targets responsible for regulating replication kinetics and coordinating replication and repair. To characterize targets of the S-phase DDR, we identified proteins phosphorylated in response to methyl methanesulfonate (MMS)-induced S-phase DNA damage in wild-type, *rad3*Δ, and *cds1*Δ cells by proteome-wide mass spectrometry. We found a broad range of S-phase–specific DDR targets involved in gene expression, stress response, regulation of mitosis and cytokinesis, and DNA replication and repair. These targets are highly enriched for proteins required for viability in response to MMS, indicating their biological significance. Furthermore, the regulation of these proteins is similar in fission and budding yeast, across 300 My of evolution, demonstrating a deep conservation of S-phase DDR targets and suggesting that these targets may be critical for maintaining genome stability in response to S-phase DNA damage across eukaryotes.

DNA damage | Rad3 | Cds1 | DDR | checkpoint

The DNA damage response (DDR) is critical for maintaining viability and genome stability in the presence of endogenous and exogenous sources of DNA damage (1). Rather than a single signal-transduction pathway, the DDR is a collection of signaling networks (2). In particular, in addition to general stress-response activities, the DDR must regulate cell-cycle–specific targets at different stages of the cell cycle. The S-phase DDR is particularly complicated because it must coordinate DNA damage repair with ongoing DNA replication. Thus, loss of the S-phase DDR leads to replication-associated genome instability (3).

The DDR is regulated primarily by conserved protein kinases (4). Damaged DNA is recognized by multiprotein complexes containing ATM, ATR, or DNA-PK, each a large, DNA-associated kinase of the PIKK family. These kinases, in collaboration with other damage-recognizing proteins and DDR-signaling mediators, directly regulate targets at sites of DNA damage (5, 6). They also activate the smaller Chk1 and Chk2 effector kinases, which are not chromatin localized and thereby coordinate the DDR throughout the cell (7).

Although these kinases are conserved from yeast to humans, their wiring is plastic (8). The S-phase DDR is activated by ATR, which responds, at least in part, to single-stranded DNA exposed by DNA damage repair and at stalled replication forks (9). In metazoans, ATR primarily activates Chk1 in response to S-phase DNA damage (7, 10). However, in the yeast S-phase DDR, ATR homologs activate Chk2 homologs—Rad53 in budding yeast and Cds1 in fission yeast (11–13). Despite this plasticity in checkpoint-kinase wiring, the biological processes regulated by the S-phase DDR are conserved.

The S-phase DDR regulates a wide range of cellular functions, including cell-cycle progression, transcription of S-phase genes, DNA-replication kinetics, and DNA repair (14, 15). However, the specific targets phosphorylated to regulate these functions have been identified in only a limited number of cases. In mammalian cells, many of these substrates are direct targets of ATR (15). In fission yeast, it is less clear if Rad3, the ATR homolog, regulates a broad range of targets directly or if most of its signaling is dependent on Cds1, the Chk2 homolog. Rad3 is known to phosphorylate histone 2A, Cds1, and the checkpoint mediator Mrc1 at sites of damage (16–18), but it has not been shown to be involved in directly phosphorylating more global targets. Moreover, the phenotype seen with the loss of both Chk1 and Cds1, the two effector kinases, in response to hydroxyurea (HU), UV, ionizing radiation (IR), and interstrand crosslinks is similar to that seen with the loss of Rad3, suggesting that much of the DDR signaling requires Chk1 and/or Cds1 (13, 19, 20).

Significance

The cellular response to DNA damage during DNA replication promotes survival and genome maintenance. It involves a network of kinases that phosphorylate a variety of target proteins. Although the protein kinases involved have been studied extensively in fission yeast, only a handful of their targets have been identified. We used an unbiased approach to profile protein phosphorylation in response to DNA damage during DNA replication. We found target proteins involved in gene expression, stress response, regulation of mitosis and cytokinesis, and DNA replication and repair, many of which are required for resistance to DNA damage. These protein targets are conserved in budding yeast and human cells, demonstrating the deep conservation of the response.

Author contributions: N.A.W., C.Z., J.M.M., A.M.C., S.J.E., and N.R. designed research; N.A.W., C.Z., J.M.M., and A.M.C. performed research; N.A.W., C.Z., A.E.H.E., S.J.E., and N.R. analyzed data; and N.A.W., A.E.H.E., A.M.C., S.J.E., and N.R. wrote the paper.

Reviewers: M.H., University of Colorado School of Medicine; and L.Z., Massachusetts General Hospital.

The authors declare no conflict of interest.

[1]Present address: Division of Hematology–Oncology, Department of Medicine, and Cancer Research Institute, Beth Israel Deaconess Medical Center and Harvard Medical School, Boston, MA 02215.

[2]N.A.W. and C.Z. contributed equally to this work.

[3]To whom correspondence may be addressed. Email: selledge@genetics.med.harvard.edu or nick.rhind@umassmed.edu.

This article contains supporting information online at www.pnas.org/lookup/suppl/doi:10.1073/pnas.1525620113/-/DCSupplemental.

To understand better the scope and organization of the S-phase DDR in fission yeast, we used phosphoproteomic profiling to identify S-phase DNA damage-induced and checkpoint kinase-dependent targets. Phosphoproteomic profiling allowed us to survey the fission yeast phosphoproteome globally using MS/MS with differentially mass-labeled samples to identify and compare directly the abundance of phosphopeptides (21). By comparing the proteins phosphorylated in an S-phase DNA damage-specific and a checkpoint kinase-specific manner, we identified several hundred targets of the S-phase DDR. Moreover, we find that these proteins are critical for the cell's survival of S-phase DNA damage and are conserved across 300 My of Ascomycete evolution.

Results

Phosphoproteomic Profiling of the S-Phase DDR in *Schizosaccharomyces pombe*. To identify proteins phosphorylated in a checkpoint-dependent manner in response to DNA damage during S phase in fission yeast, we identified phosphopeptides induced by DNA damage in S-phase–synchronized cells and compared them with phosphopeptides induced by damage in DDR-kinase mutant cells. Specifically, we compared results from cells lacking Cds1, the Chk2 kinase ortholog, which is specific for S-phase damage signaling in fission yeast (13), and cells lacking Rad3, the ATR ortholog, which is required for the great majority of DDR signaling in fission yeast (22, 23). We also compared these results with phosphopeptides from cells treated with DNA damage during G2 and cells arrested in S phase by the replication inhibitor HU. Altogether, we collected seven phosphoproteomic datasets, the details of which are presented in Dataset S1, Table S1.

We first identified S-phase DNA damage-induced phosphopeptides by comparing cells treated or not treated with DNA damage during S phase. We treated S-phase cells with 0.03% methyl methanesulfonate (MMS), a dose that slows bulk replication in a Cds1-dependent manner (Fig. S1) (13). Cells were harvested in mid-S phase and analyzed by phosphopeptide-enriched MS, as detailed in *Materials and Methods* and diagrammed in Fig. 1*A*. Briefly, cells arrested in early G1 were selected by centrifugal elutriation and were released into a synchronous S phase in the presence or absence of MMS. Because these cells have intact DDRs, we refer to them as "wild-type cells." S-phase progression was monitored by flow cytometry, and samples were taken for phosphoproteomic analysis in mid-S phase (Fig. S1). Protein was isolated, digested with trypsin, and enriched for phosphopeptides by affinity chromatography. Peptides were analyzed by LC-MS/MS, and those that passed our quality filters were quantitated using the Vista algorithm (24). We identified 7,132 phosphopeptides representing 2,320 unique peptide sequences in 1,075 proteins. Of these proteins, 298 contain phosphopeptides that were enriched at least twofold in the damaged sample. We refer to the resulting dataset as "WT-MMS" (Dataset S1, Tables S1–S3).

We next identified S-phase phosphopeptides from damage-treated cells that were dependent on the S-phase checkpoint kinase Cds1. Using the approach described above, we compared phosphopeptides generated in MMS-treated wild-type cells with those generated in MMS-treated *cds1*Δ cells (Fig. 1*A* and Fig. S1). We identified 9,442 phosphopeptides representing 2,987 unique peptide sequences in 1,293 proteins. Of these proteins, 459 contain phosphopeptides that were enriched at least twofold in the wild-type sample. We refer to the resulting dataset as "Cds1-MMS" (Dataset S1, Tables S1–S3). Comparing the S-phase damage-induced and Cds1-dependent phosphopeptides, we identified 209 of those proteins that are phosphorylated in response to S-phase DNA damage in a Cds1-dependent manner (Fig. 1*B*).

To investigate the extent to which Cds1-independent phosphopeptides might be direct or indirect targets of Rad3, we repeated the experiment with *rad3*Δ cells (Fig. 1 and Fig. S1). We identified 2,595 phosphopeptides representing 1,014 unique peptide sequences in 640 proteins. Of these proteins, 200 contain phosphopeptides that were enriched at least twofold in the wild-type sample. We refer to the resulting dataset as "Rad3-MMS"

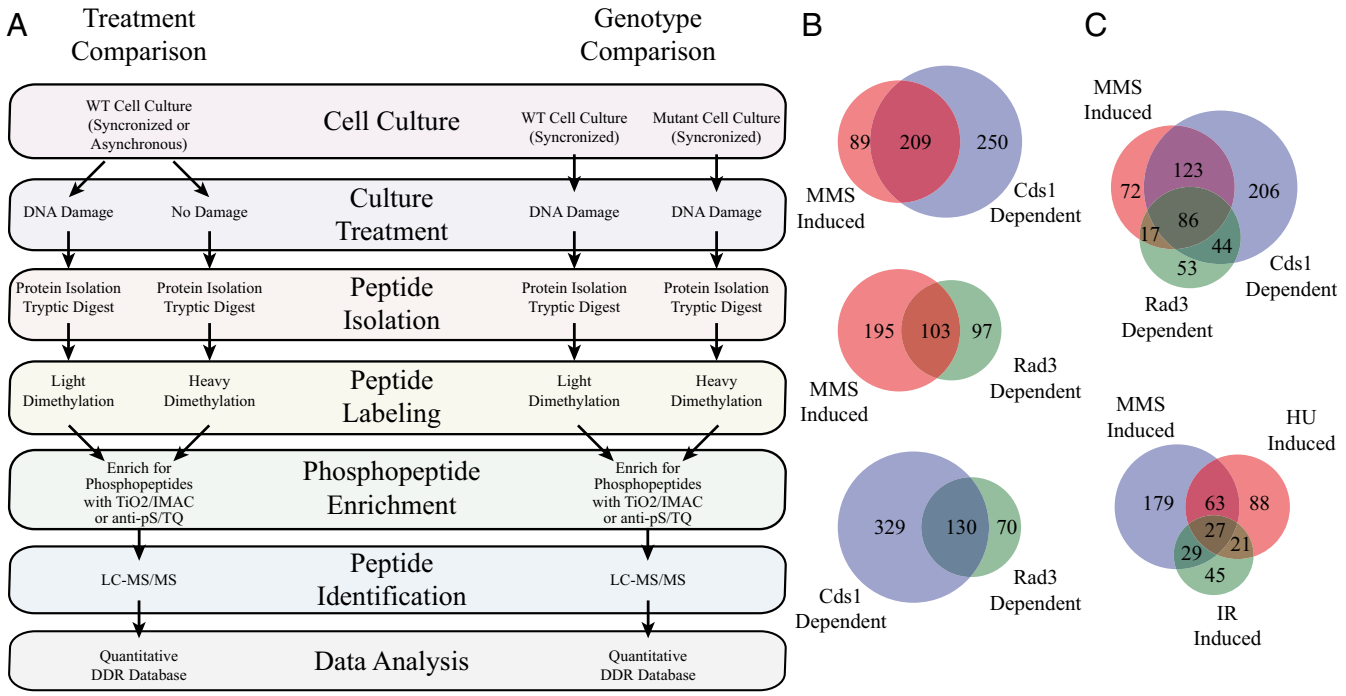

Fig. 1. Experimental design and identified phosphopeptides. (*A*) The workflow of our phosphopeptide-profiling experiments. (*B*) Two-way overlap between phosphorylated proteins identified in our MMS-induced (WT-MMS), Cds1-dependent (Cds1-MMS), and Rad3-dependent (Rad3-MMS) datasets. (*C*) Three-way overlap between phosphorylated proteins identified in our MMS-induced (WT-MMS), Cds1-dependent (Cds1-MMS), and Rad3-dependent (Rad3-MMS) datasets and our MMS-induced (WT-MMS), HU-induced (WT-HU), and IR-induced (WT-IR) datasets.

(Dataset S1, Tables S1–S3). The majority (65%) of Rad3-dependent phosphoproteins are also Cds1 dependent (Fig. 1*B*), consistent with the idea that most Rad3 signaling during S phase goes through Cds1. Moreover, only 7% (18/243) of the unique Rad3-dependent twofold-enriched phosphopeptides were phosphorylated on SQ or TQ, the Rad3 target motif.

Although there is significant overlap between the Cds1- and Rad3-dependent targets, a number of phosphorylation events were present in either the Cds1-MMS dataset or the Rad3-MMS dataset but not both datasets. Many of these proteins may be phosphorylated in both a Cds1- and Rad3-dependent manner but are missing from one of the datasets because of experimental variability in detection by mass spectrometry. In particular, the presence of targets that appear in the Cds1-MMS dataset but not the Rad3-MMS dataset may result from the smaller size of the latter. However, some of the Rad3-dependent phosphorylations that are still phosphorylated in *cds1*Δ cells may be targets of Chk1, which is activated by S-phase DNA damage in *cds1*Δ cells (13, 25) and phosphorylates some of the same substrates as Cds1 (26). Nonetheless, because Chk1 is not activated during the S phase in wild-type cells (13, 25), these substrates are unlikely to be physiological targets of Chk1.

To explore further the possible direct targets of Rad3, we employed immuno-enrichment of phospho-SQ (pSQ)–containing peptides, a technique which should identify less abundant peptides (15). In one experiment, we compared pSQ-enriched peptides in MMS-treated and -untreated S-phase cells, producing the dataset WT-pSQ. We then compared pSQ-enriched peptides in MMS-treated S-phase wild-type and *rad3*Δ cells, producing the dataset Rad3-pSQ (Fig. 1*A* and Fig. S1). We recovered many fewer phosphopeptides in these experiments: 142 and 187, representing 68 and 77 unique sequences in 62 and 72 proteins, respectively, of which 27 and 12 were enriched at least twofold (Dataset S1, Tables S1–S3).

We reasoned that the DDR-dependent DNA damage-induced phosphopeptides we identified in S-phase cells would comprise both S-phase damage-specific targets and more general DDR targets. To discriminate between the two, we identified targets of S-phase DDR signaling induced by HU, which triggers cell-cycle arrest by preventing dNTP synthesis and thus arresting DNA polymerases without causing DNA damage per se, and G2 DDR signaling induced by IR, which causes a DNA damage-induced G2 arrest. From the comparison between HU-treated and -untreated cells (dataset WT-HU), we identified 9,057 phosphopeptides representing 3,705 unique sequences in 1,905 proteins, 209 of which were enriched at least twofold in response to HU treatment. From the comparison between irradiated and unirradiated cells (dataset WT-IR), we identified 7,961 phosphopeptides representing 3,266 unique sequences in 1,797 proteins, 122 of which were enriched at least twofold by IR treatment. Many of the HU- and IR-induced peptides overlap with those induced by MMS, although the overlap is notably less than the overlap among the three MMS-treated datasets (Fig. 1*C*).

In total, we identified 33,973 unique phosphopeptides, 2,068 of which, in 726 proteins, were enriched at least twofold in one or more datasets. A summary of the seven datasets is presented in Dataset S1, Table S1. The complete S-phase DDR phosphoproteomic database is provided in Dataset S1, Table S2 and Dataset S2. Proteins with phosphopeptides that are enriched at least twofold in any dataset are listed in Dataset S1, Table S3.

Assessment of the Quality of the Phosphoproteomics Datasets. We assessed the quality of our phosphoproteomic database using several comparative metrics. First, we examined the reproducibility of our data using an internal control. As a result of our experimental strategy—which involves differentially mass-labeling and mixing control and experimental samples, identifying peptides in the mass spectrometer, and then looking for their differentially mass-labeled cognate—we often independently isolate a heavy peptide and compare it with its light cognate in one MS cycle and then independently isolate the light version and compare it with its heavy cognate in a subsequent cycle. A comparison of these two measurements reveals how reproducible our measurements are and how much noise we introduce during the LC-MS/MS procedure. Across all datasets, the median difference in calculated enrichment ratios between independent phosphopeptide identifications is 0.0051, demonstrating that our enrichment estimates are highly reproducible (Fig. 2*A*).

As another indication of specificity, we compared the enrichment of phosphorylated RxxS sequences, a known consensus target of Cds1 (27), in our datasets. The WT-MMS and Cds1-MMS datasets both show significant enrichment of RxxpS in their

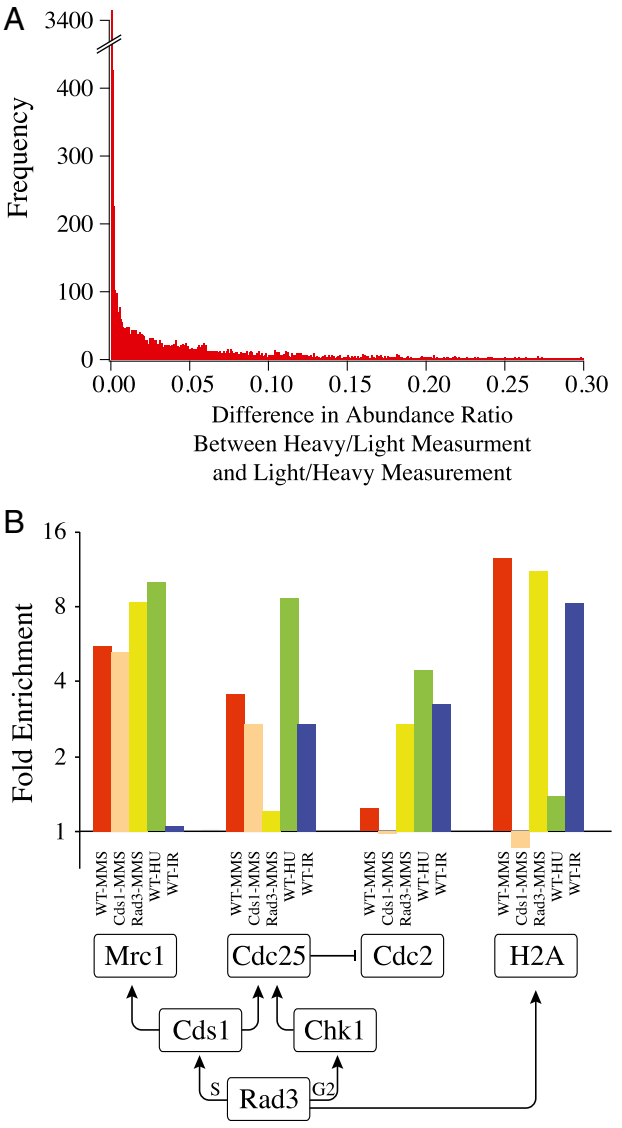

Fig. 2. Quality assessment of phosphopeptide datasets. (*A*) The distribution of differences in Vista ratios (the ratio of peptide abundances in the control and experimental samples) when two nominally identical measurements were compared: the Vista ratio when the light-labeled peptide was identified first vs. the Vista ratio when the heavy-labeled peptide was identified first. The mean for the distribution is 0.043, and the median is 0.0051. (*B*) Enrichment across all datasets of four well-characterized phosphoproteins: Mcr1, Cdc25, Cdc2, and histone 2A. A diagram of the checkpoint kinase circuit is shown below the graph.

fourfold-enriched phosphopeptides ($P = 2.6 \times 10^{-2}$ and 1.3×10^{-5}, respectively, Fisher's exact test). Likewise, SQ-containing phosphopeptides are highly enriched in the pSQ affinity datasets. For WT-pSQ, 114/142 (80%) of phosphopeptides contain an SQ or TQ; for Rad3-pSQ the ratio is 167/187 (89%).

Another indication of the quality of our datasets is the inclusion of known S-phase DDR phosphorylation targets. Three of the best-studied phospho-targets downstream of Cds1 are the Mrc1 mediator, the Cdc25 phosphatase, and its target, the Cdc2 cyclin-dependent kinase, DDR regulation of which prevents cell division during activation of the checkpoint (22, 26, 28–30). The WT-MMS, Cds1-MMS, Rad3-MMS, WT-HU, and WT-IR datasets all contain at least twofold-enriched phosphopeptides for Mrc1, Cdc25, and/or Cdc2 (Fig. 2*B*). The low level of Mrc1 in the WT-IR dataset is expected because Mrc1 phosphorylation is specific to S phase. In addition, the low level of Cdc2 phosphorylation in the WT-MMS and Cds1-MMS datasets is expected because Cdc2 is normally phosphorylated when complexed with Cdc13 in S phase and G2; checkpoint activation simply maintains that phosphorylation. Cdc2 phosphorylation is increased in the WT-HU and WT-IR datasets because those cells were checkpoint arrested, allowing Cdc13 to accumulate and thus producing more Cdc2–Cdc13 to be phosphorylated. Another known S-phase DDR target, the γ-H2A phosphopeptide, a well-studied direct Rad3 target (16, 31), is enriched at least eightfold in the WT-MMS, Rad3-MMS, and WT-IR datasets (Fig. 2*B*). Consistent with this phosphorylation being Rad3- but not Cds1-dependent and with γ-H2A not being phosphorylated in response to HU above normal S-phase levels, the phosphopeptide is not enriched in the Cds1-MMS or WT-HU datasets (32). All in all, we find the expected pattern of phosphorylation in the four proteins in 18 of 20 cases across the five datasets. The two exceptions are the low Cdc25 phosphorylation and high Cdc2 phosphorylation in the Rad3-MMS dataset. We ascribe these exceptions to experimental variability, possibly resulting from the smaller size of the Rad3-MMS dataset.

Finally, we examined the overlap between damage-induced and DDR kinase-dependent S-phase phosphopeptides, which should be extensive. As expected, in each two-way comparison a majority of the smaller dataset overlaps with the larger dataset: 209/298 (70%) for WT-MMS vs. Cds1-MMS, 103/200 (52%) for WT-MMS vs. Rad3-MMS, and 130/200 (65%) for Cds1-MMS vs. Rad3-MMS (Fig. 1*B*).

Analysis of Damage-Induced and Checkpoint-Dependent Phosphorylation Sites. To investigate which kinases may be activated by S-phase DNA damage and to explore the specificity of Cds1- and Rad3-dependent phosphorylations, we analyzed the sequence context of our up-regulated phosphorylations. We used the Motif-X program to identify enriched sequence motifs in our dataset, using the *S. pombe* proteome as the background (33).

In our WT-MMS dataset we find three significantly enriched phosphorylation motifs in our twofold up-regulated phosphopeptides: RxxpS, pSP, and pSD (Fig. 3). The RxxpS-phosphorylated phosphopeptides are presumed to be direct targets of Cds1 (27). SP is the known recognition target of both the CDK and MAP family of kinases; SD is phosphorylated by kinases of the CK2 family. Although we have no direct evidence of their involvement in MMS-induced S-phase phosphorylation, the Sty1 MAP and Cka1 CK2 kinase are both involved in cell-cycle and cell-growth control and could plausibly be responsible for S-phase DNA damage-induced phosphorylations.

To determine if the non-Cds1 phosphorylations we observe are caused by DDR-independent responses to MMS or to other kinases activated by Cds1, we examined the sequence context of the phosphorylations up-regulated twofold in our Cds1-MMS and Rad3-MMS datasets. In both datasets, we saw the same range of motifs and extensive substrate overlap with the WT-MMS dataset

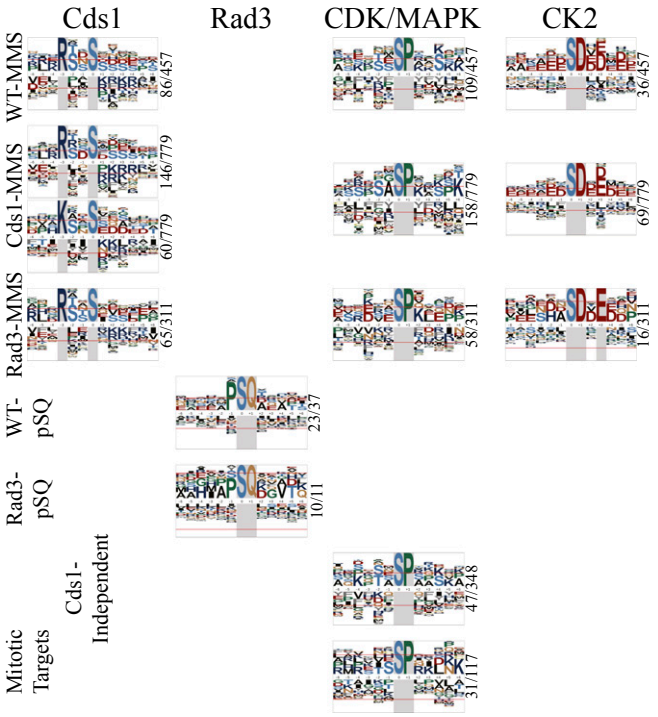

Fig. 3. Phosphopeptide motif enrichment. Enriched phosphosite motifs identified by the Motif-X algorithm (33, 34). The residues in gray are the fixed positions defining the motif. At other positions, enriched and depleted residues are shown above and below the midline, respectively. The red lines indicate statistical significance at the 0.05 level. The Cds-1–independent phosphopeptides are those found in the WT-MMS dataset but not in the Cds1- or Rad3-MMS datasets. The mitotic target phosphopeptides are those found in the WT-MMS dataset but not in the Cds1- or Rad3-MMS datasets and that have mitotic GO annotations.

(Figs. 1 and 3). These results suggest that the majority of S-phase phosphorylations induced by DNA damage are caused, directly or indirectly, by the activation of Rad3 and Cds1. However, if we look specifically at the peptides phosphorylated in a DDR-independent manner (those enriched at least twofold in the WT-MMS dataset but not in the Cds1-MMS or Rad3-MMS datasets), we find they are not enriched for the RxxpS motif ($P = 0.46$) but instead are enriched for the pSP motif, consistent with checkpoint-independent CDK or MAP kinase phosphorylation (Fig. 3).

Because the S-phase DDR is dependent on Rad3, we were surprised to find no enrichment in pSQ phosphorylations in the phosphopeptides up-regulated twofold in either the WT-MMS or Rad3-MMS dataset ($P = 0.15$ and 0.09, respectively, Fisher's exact test). This result suggests that most of the Rad3-dependent phosphorylations are regulated indirectly through Cds1 and other downstream kinases. Alternatively, Rad3 SQ substrates may tend to be less abundant than Cds1 substrates. However, pSQ is the motif identified in the pSQ datasets (Fig. 3), indicating that additional direct Rad3 substrates might be found were the proteome to be sampled more deeply. Importantly, we observe a significant enrichment for proline preceding the pSQ site, with 11/37 ($P = 8.7 \times 10^{-8}$, Fisher's exact test) pSQ peptides in the WT-pSQ dataset and 4/11 ($P = 5.0 \times 10^{-4}$) in the Rad3-pSQ dataset being PpSQ motifs. As far as we are aware, PpSQ has not been seen previously for other PIKK kinase extended-recognition motifs, but the fact that it was seen in a dataset derived from antibody enrichment leaves open the possibility that the antibodies used favor prolines in that position rather than the kinases themselves.

DDR-Dependent Phosphorylations Span a Diverse Spectrum of Biological Functions. The phosphoproteins identified in our datasets span a broad range of biological functions. To investigate which biological processes are preferentially targeted by S-phase DNA damage- and S-phase checkpoint kinase-dependent phosphorylation, we calculated which gene ontology (GO) categories are enriched in each of our datasets (35). Our S-phase DNA damage datasets (WT-MMS, Cds1-MMS, and Rad3-MMS) are enriched in annotated GO terms that fall into several broad categories—gene expression, cytoskeleton and cytokinesis, signal transduction, stress response, cell cycle, and DNA repair—with the bulk of the phosphorylated protein being associated with gene expression or cytoskeleton and cytokinesis (Fig. 4*A* and Dataset S1, Table S4).

Phosphorylation by the S-phase DDR of proteins involved in gene expression is pervasive. We find four major classes of gene expression-related proteins enriched in our S-phase DNA damage

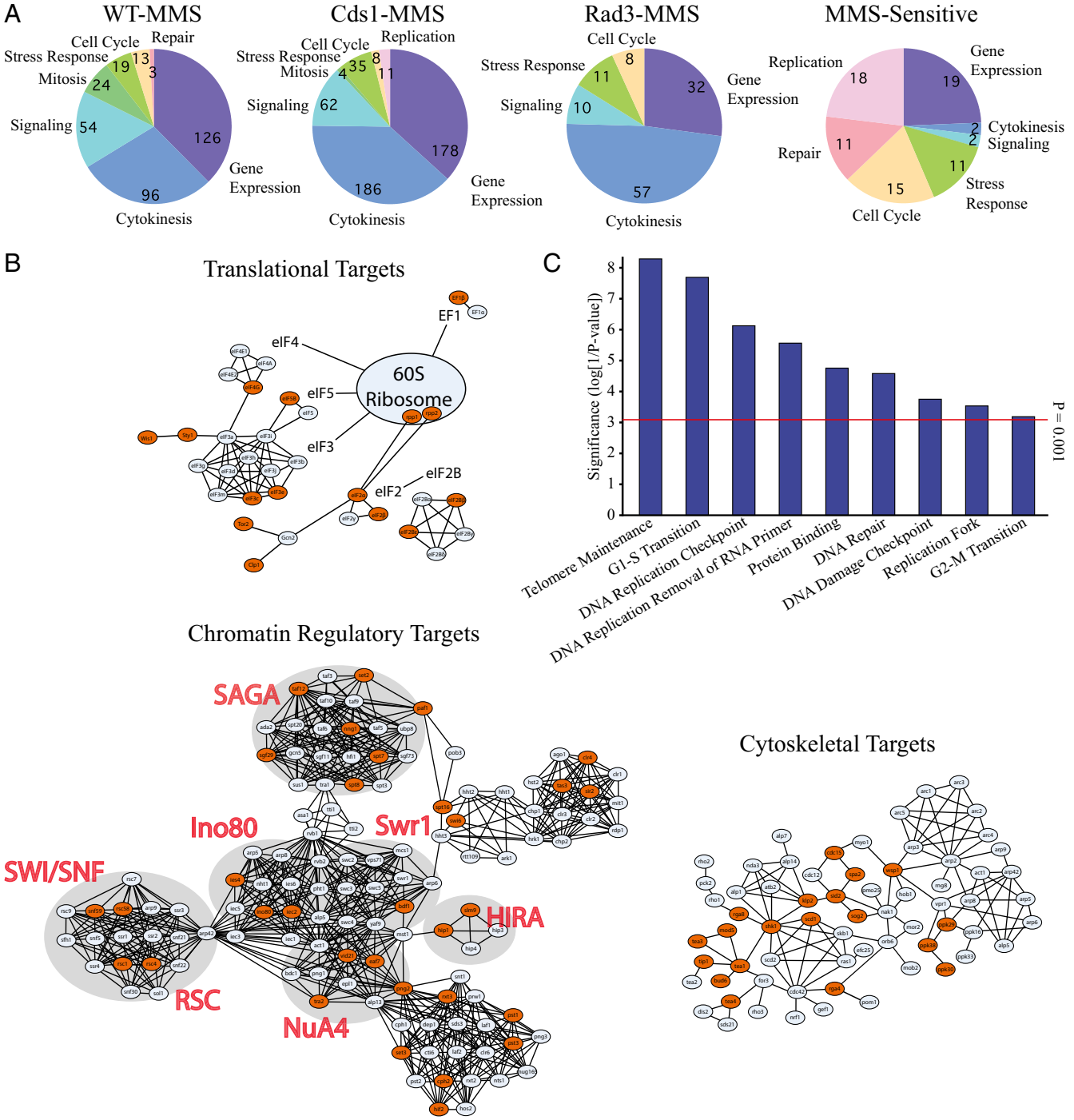

Fig. 4. Biological classification of enriched phosphoproteins. (*A*) GO enrichment for the three MMS datasets and for the S-phase DDR targets that are required for MMS resistance. (*B*) Clustergrams for networks of proteins involved in translation, chromatin, and the actin cytoskeleton; S-phase DDR targets are shown in orange. Networks are based on interaction data from BioGRID and manual curation from PomBase and were visualized with esyN (43, 61, 62). (*C*) Statistical significance of the enrichment of GO terms for the DDR targets required for resistance to MMS (43, 44). All GO terms with $P < 10^{-3}$ are included.

datasets: chromatin modification, transcription, mRNA processing, and translation (Fig. 4*A* and Dataset S1, Table S5). The 43 genes involved in chromatin modification include histone-modifying enzymes such as methyltransferases, demethylases, acetylases, and deacetylases and chromatin remodeling complex subunits of the Fun30, SAGA, Ino80, RSC, and SWI/SNF families (Fig. 4*B*). Chromatin remodeling complexes, in particular Ino80, RSC, and SWI/SNF, are implicated in DNA damage repair (36), suggesting that these S-phase DDR targets also could be directly involved in the repair of the MMS lesions. The 63 genes involved in transcription include gene-specific transcription factors, such as the Fkh1, Fhk2, and Sep1 forkhead proteins, which regulate mitosis and cytokinesis, Nrm1, a known target of Cds1 (37, 38), and a number of basal transcription factors, including subunits of TFIID, TFIIF, and the transcriptional elongation factor TFIIS. The 57 genes involved in mRNA processing include proteins involved in mRNA export, several components of the spliceosome, and many uncharacterized RNA-binding proteins. Nine of the 11 genes involved in translation include are subunits of the eIF2, eIF3, and eIF4 translation initiation factor complexes, suggesting that the S-phase DDR has a direct effect on translational initiation, perhaps via indirect regulation through the Wis1–Sty1 stress MAP kinase pathway or via Clp1, a strong target (enriched 6.3- to 16.7-fold) in all three S-phase DNA damage datasets, and Tor1, a weak target (enriched 1.9- to 2.0-fold) in all three datasets (Fig. 4*B*). Taken together, these targets suggest that the S-phase DDR regulates gene expression on multiple levels and in both gene-specific and transcriptome-wide manners.

The S-phase DDR also phosphorylates a wide range of proteins associated with cytoskeletal and cytokinetic GO terms. These proteins fall into four broad, overlapping classes: the actin cytoskeleton, the septum, the cell tip, and cellular polarity (Fig. 4*A* and Dataset S1, Table S6). The 12 genes involved in the actin cytoskeleton include direct regulators of actin dynamics, such as WASP and several Prk-family kinases, and regulators of cortical patch formation, such as espin homologs. Interestingly, the cytoskeletal DNA damage- and DDR kinase-dependent targets are primarily actin-cytoskeletal and include very few microtubule-cytoskeletal proteins. However, as described below, microtubule-cytoskeletal proteins are phosphorylated in a damage-dependent but DDR kinase-independent, manner. The 81 genes involved in the septum include both regulators of septum location and function, such as Gin4-family kinases and GTPase-activating proteins, and proteins involved in septum synthesis, such as contractile ring proteins and β-glucan synthases. The 42 genes involved in the cell tip include tip-regulatory proteins, such as Tea1, Tea3, and Tip1, and many more general actin-cytoskeletal regulatory proteins that overlap with the septum class of proteins (Fig. 4*B*). Most of the 12 genes involved in cellular polarity are actin-cytoskeletal regulatory proteins that overlap with the other three classes.

The final classes of enriched S-phase DDR targets are signal transduction, stress response, and cell cycle. As expected for a protein–kinase network, most of the proteins annotated as being involved in signal transduction are protein kinases; many are known or presumed down-stream targets of Cds1, such as Cdc2, the Hsk1 replication kinase, the Plo1 Polo kinase, and the Sty1, Srk1, Wis1, and Win1 stress MAP kinases, but there are many uncharacterized kinases, as well. However, the signal transduction class also includes regulators of cytoskeletal dynamics, which overlap with the cytoskeletal and cytokinetic class of proteins. In addition to the stress MAP kinases, the stress response class of proteins includes protein chaperones and ubiquitin-binding proteins. The cell cycle class of proteins includes the well-studied Cds1-dependent substrates Cdc25, Cdc2, Mrc1, Cdc18, and Hsk1.

Two categories of proteins are differentially phosphorylated in the S-phase DNA damage-dependent (WT-MMS) and S-phase checkpoint kinase-dependent (Cds1-MMS and Rad3 MMS) datasets (Fig. 4*A*). The first category comprises mitotic proteins, whose phosphorylation is damage dependent but DDR independent. These proteins include regulators of mitotic progression, such as the Bub1 kinase, the Plo1 Polo kinase, the Nak1 PAK kinase, and the mitotic exit phosphatase Clp1; proteins involved in cohesion, such as the Rad21 kleisin subunit of cohesin and the Mis4 subunit of the cohesin loader; and spindle-pole-body proteins, such as the Pcp1 pericentrin homolog and the Sif1 spindle-pole-body protein. The fact that these proteins are not found in the DDR kinase-dependent datasets suggest that they may be phosphorylated by other kinases in response to the general stress caused by non-DNA targets of MMS alkylation instead of by the DDR kinase-dependent response to MMS-induced DNA damage (39). Consistent with this possibility, they are not enriched for the RxxpS motif ($P = 0.29$); instead, they are enriched for the pSP motif, consistent with Sty1 stress kinase phosphorylation (Fig. 3).

The second category is replication proteins, for which phosphorylation is DDR kinase dependent [being significantly enriched in Cds1-MMS ($P = 0.019$) and modestly enriched in Rad3-MMS ($P = 0.17$)] but not damage dependent [being unenriched in WT-MMS ($P = 0.52$)]. These proteins appear to be constitutively phosphorylated in a Rad3- and Cds1-dependent manner in the absence of DNA damage. They include proteins intimately involved in Cds1 function, such as Mrc1 and Drc1; proteins with more general roles in DNA replication, such as Cdc6 (the catalytic subunit of pol δ) and Pfh1, (the Pif1 helicase homolog); and proteins specifically involved in Okazaki-fragment maturation, such as Cdc17 (DNA ligase), Rad2 (the FEN1 flap endonuclease homolog), and Rnh1 (RNase H). These proteins are significantly enriched in RxxS-containing peptides ($P = 4.3 \times 10^{-3}$), suggesting that many are directly phosphorylated by Cds1. These proteins appear to be phosphorylated in a Cds1-dependent but damage-independent, manner, consistent with evidence from other systems that the S-phase DDR kinases have critical roles in regulating replication in unperturbed S phase (40–42).

DDR-Dependent Phosphoproteins Are Enriched for Proteins Required for DNA Damage Resistance. Having identified a large number of proteins phosphorylated in response to S-phase DNA damage, we tested how many of these proteins contributed to resistance to MMS-induced DNA damage. Two hundred forty-one fission yeast genes have been identified as having an MMS-sensitive mutant phenotype (43, 44). Of these, a significant fraction are phosphorylated in a Cds1-dependent manner (36/241, $P = 1.7 \times 10^{-3}$, hypergeometric test) (Dataset S1, Table S3). These proteins are highly enriched for proteins involved in DNA replication, DNA repair, and cell-cycle control ($P < 10^{-3}$, hypergeometric test) (Fig. 4*C*). Instructive examples include Cdc25, regulation of which is known to be required for DNA damage resistance because of its role in preventing damaged cells from entering mitosis; the recombinational mediator Rad52 and the repair helicase Pfh1, which are required for DNA damage repair; and the stress kinases Sty1 and Wis1. These results suggest that Cds1 regulates proteins that are known to be important in the cellular response to S-phase DNA damage and that this regulation is important for cells' ability to survive S-phase DNA damage.

Fission Yeast DDR-Dependent Phosphoproteins Are Conserved in Budding Yeast and Humans. It is expected that the general categories of proteins regulated by the S-phase DDR, such as DNA replication, DNA repair, and cell-cycle control, would be similar across organisms. However, it is not clear that the same proteins must be regulated, especially because, as discussed in the Introduction, the wiring of the DDR kinases is not completely conserved. To test if the specific targets of the S-phase DDR are conserved, we examined the frequency of overlap in S-phase DDR targets in our fission yeast data and in budding yeast data,

the only other organism for with such data are available. There are 242 budding yeast proteins with fission yeast orthologs reported to be phosphorylated in response to MMS-induced S-phase DNA damage (45). Almost half of these proteins (115/242) are enriched in our MMS datasets ($P < 10^{-10}$, hypergeometric test) (Fig. 5*A* and Dataset S1, Tables S3 and S8). Comparison with a previous budding yeast S-phase DDR-phosphoproteomic dataset yielded a similar result (17/45, $P < 3.8 \times 10^{-3}$) (46). The proteins that are phosphorylated in both species fall into the same categories as those phosphorylated in fission yeast (Fig. 5*B*), the notable exceptions being mitotic and cell-cycle regulation, consistent with the two species having different mechanisms for regulating the entry into mitosis.

Although S-phase–specific DDR phosphoproteomic datasets are not available for metazoans, there are datasets in which asynchronous human cells have been treated with UV radiation, which triggers the S-phase DDR in the replicating cells in the culture (47). To determine if similar targets are phosphorylated by the S-phase DDR in humans and fission yeast, we calculated the enrichment of orthologous proteins in the human UV datasets and our MMS datasets. The human UV dataset contains 1,182 unique proteins, 179 of which contain at least one peptide that is enriched twofold in response to UV radiation. Of those proteins, 66 have fission yeast orthologs. We found significant overlap among our WT-MMS, Cds1-MMS, and Rad3-MMS datasets (Fig. 5*C* and Dataset S1, Tables S3 and S9). As a specificity control, we performed the same comparison with a parallel human dataset from IR-treated cells (47) and found no significant overlap among targets.

The S-phase DDR targets shared between fission yeast and humans are most heavily enriched in proteins implicated in gene expression (Dataset S1, Table S9). These proteins include Clr6 and RSC complex subunits, Spt5 transcriptional elongation factor, U2 snRNP and U3 snoRNP subunits, and other splicing and RNA-binding proteins. In addition three nucleoporins—NUP98/Nup189, NUP153/Nup124, and NUP35/Nup40—and the Sbp1 Ran Gap are targeted in both species. Other gene categories seen in the fission yeast data that also are targeted in human cells including cytokinesis (anillin), signaling (PI kinase Tra2), mitosis (Mis4 cohesin loader), repair (histone H2AX), and replication

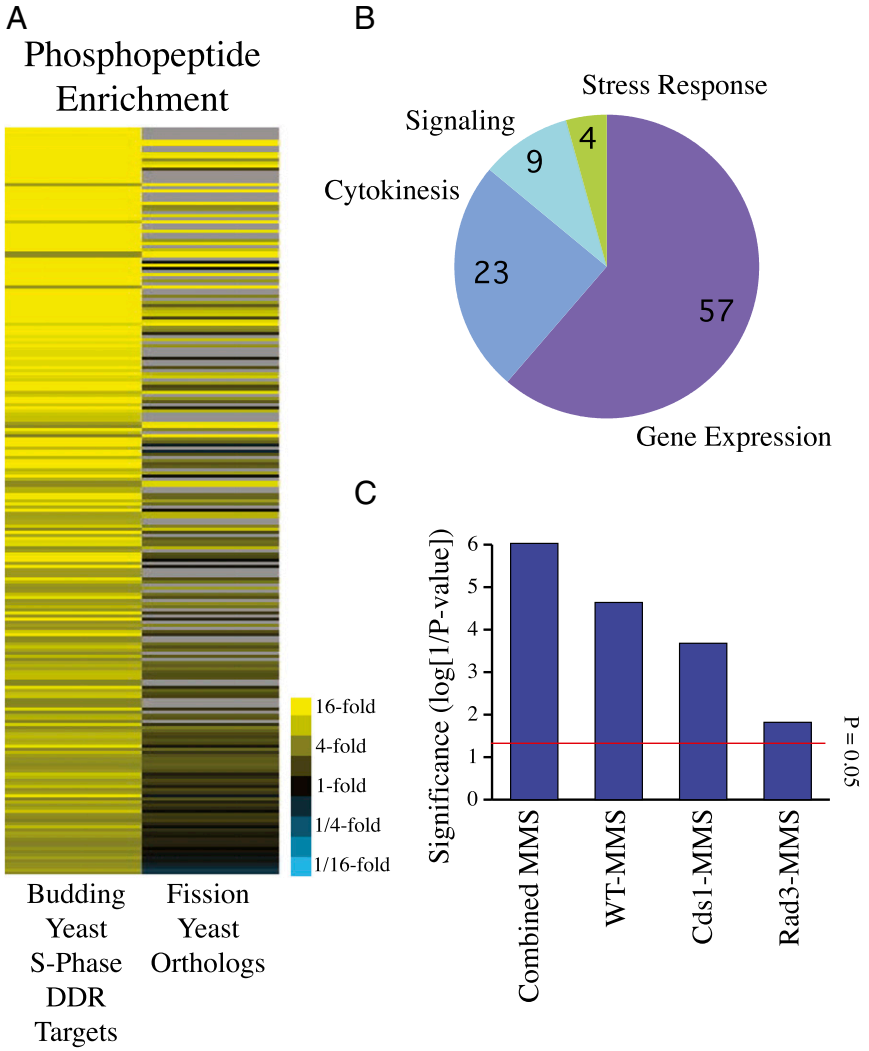

Fig. 5. Conservation of S-phase DDR Targets. (*A*) A heat map of the S-phase DDR targets conserved between budding yeast and fission yeast. Budding yeast S-phase DDR targets with fission yeast orthologs and the corresponding fission protein are ranked by average enrichment (45). Gray indicates that the fission yeast homolog was not detected in our datasets. (*B*) GO enrichment for homologs that are S-phase DDR targets in both budding and fission yeast. (*C*) Statistical significance of the overlap between human DDR targets phosphorylated in response to UV radiation (47) and their fission yeast homologs phosphorylated in the indicated datasets. "Combined MMS" refers to the WT-, Cds1-, and Rad3-MMS datasets combined.

(Rfc1) (Dataset S1, Table S9). The two categories that are not represented are stress response and cell cycle. The broad distribution of S-phase DDR targets conserved between fission yeast and both budding yeast and humans suggests a deep conservation of the DDR signaling networks.

Discussion

We have taken a proteome-wide approach to identify proteins phosphorylated by the fission yeast S-phase DDR. This signaling network has been well characterized, and its central kinases, the ATR homolog Rad3 and the Chk2 homolog Cds1, have been studied extensively. Nonetheless, although several specific targets are known, little is known about the network at the systems level. For instance, the extent to which Rad3 regulates downstream targets directly or indirectly through Cds1 is unclear, as is the extent to which Cds1 activates downstream kinases to effect the S-phase DDR. Our data also allowed us to investigate the conservation of S-phase DDR targets by comparing our data with that from budding yeast and human cells.

The sequence motifs of the up-regulated phosphorylations and their kinase dependence provide insight into which kinases are responsible for phosphorylating S-phase DDR targets. Rad3, the fission yeast ATR homolog, is genetically required for S-phase DDR (23). Direct Rad3 targets can be identified by the distinctive S/TQ recognition site for the PIKK family of protein kinases including ATR, DNA-PK, and ATM in mammals (48). We did find potential direct Rad3 targets, but only about 10% as many as non-SQ targets, in our general S-phase DNA damage datasets (WT-MMS, Cds1-MMS, and Rad3-MMS) and in our other DDR datasets (WT-HU and WT-IR), suggesting that Rad3 regulates most of the S-phase DDR indirectly via Cds1, which is the fission yeast S-phase DDR effector kinase and Chk2/Rad53 homolog.

Because Tel1, the fission yeast ATM homolog, phosphorylates many of the same substrates as Rad3, it may substitute for Rad3 in our Rad3-MMS and Rad3-pSQ datasets, obscuring Rad3's direct targets. However, Rad3 and Tel1 substrates still would be expected to appear in our other datasets, which are not Rad3 specific. Moreover, Tel1 cannot substitute for Rad3 in the activation of Cds1 in response to MMS (49), demonstrating that at least some of Rad3's critical targets are not phosphorylated efficiently by Tel1. Finally, Rad3's best-characterized target, the C terminus of histone 2A, which also is phosphorylated by Tel1 (16), appears in our Rad3-MMS and Rad3-pSQ datasets, demonstrating that, in response to S-phase DNA damage, histone 2A phosphorylation is primarily Rad3 dependent. This result is in contrast to findings in mammals treated with IR, in which a significant proportion of regulated phosphosites are SQ (15). Taken together, these results suggest that Rad3 has a limited repertoire of direct S-phase DDR targets and that a large portion of S-phase DDR signaling is amplified through Cds1. Nonetheless, we do find potential novel Rad3 targets, including the Hus1 checkpoint-clamp subunit and the Cdc6 DNA polymerase δ catalytic subunit.

Consistent with the conclusion that Rad3 acts largely through Cds1, many of the S-phase DDR targets are phosphorylated on RxxS, the Cds1 recognition motif (Fig. 3) (27). However, many are phosphorylated on other sites, in particular SP, which is targeted by CDK and MAP kinases, and SD, indicating phosphorylation by CK2 family kinases (50). Because the activity of Cdc2, the fission yeast CDK, is prevented from increasing by the S-phase DDR (12, 13, 28), Cdc2 is unlikely to be responsible for the increase in SP phosphorylation. The Sty1 stress-activated MAP kinase is a plausible candidate for the SP-directed phosphorylation, because Sty1 is known to be activated by MMS treatment (51). Many of the SP- and SD-directed phosphopeptides appear in both our WT-MMS and Cds1-MMS datasets, suggesting that they are indirect targets of Cds1 and are phosphorylated by kinases that are activated in a Cds1-dependent manner. However, some phosphopeptides are not found in our Cds1-MMS or Rad3-MMS datasets, suggesting that they are not DDR kinase dependent. These phosphopeptides are enriched in SP target sites, suggesting that many may be Sty1 targets. DDR kinase-independent MAP kinase activation in response to MMS-induced damage would be reminiscent of UV-induced activation of MAP kinase in enucleated mammalian cells (52, 53) and would suggest that in yeast, too, broad-spectrum damaging agents, such as UV and MMS, can activate stress-response pathways in response to non-DNA damage, possibly to RNA, protein, or other cellular components. Of course, we cannot rule out the possibility that a branch of kinase signaling may be independent of the known DDR kinases but nonetheless dependent on DNA damage.

Finally, we identified proteins that are phosphorylated in a Cds1-dependent manner, whether the cells were damaged or not. These proteins, which appear in our DDR kinase-dependent datasets (Cds1-MMS and Rad3-MMS) but not in our S-phase damage-dependent dataset (WT-MMS), presumably are phosphorylated in S phase in response to endogenous DNA damage, other constitutive replication stress, or basal activity of the DDR kinases. These proteins are enriched in components of the replication fork, suggesting that they primarily regulate the local replication machinery rather than broader cellular functions. ATR is essential in many organisms, as is Rad53 in budding yeast, because of its constitutive role in DNA replication (40, 42, 54). Fission yeast is unusual in that Rad3 or Cds1 is not required for viability, but their damage-independent targets suggest that they, too, have constitutive roles in regulating DNA replication.

The proteins phosphorylated in response to S-phase DNA damage span a broad range of biological functions. Nonetheless, most are in the gene expression or cytoskeleton and cytokinesis categories, suggesting a broad change in gene-expression and cell-growth programs. Interestingly, we see only a modest enrichment of the gene classes involved in cell-cycle control, DNA replication, and DNA repair (Fig. 4*A*). However, that observation does not mean there are no important targets in those gene classes. For instance, if one or two critical cell-cycle proteins are regulated, they may be central to the biological function of the S-phase DDR but not sufficiently abundant to be identified by gene-enrichment analysis. An evaluation of the S-phase DDR targets important for MMS resistance supports this possibility. Of the 241 fission yeast genes annotated as required for MMS resistance (43, 44), a significant number (36, $P = 1.7 \times 10^{-3}$) (Dataset S1, Table S3) appear in our S-phase DNA damage datasets (WT-MMS, Cds1-MMS, and Rad3-MMS). However, instead of being enriched in cytokinesis or cytoskeletal annotations, these S-phase DDR targets are highly enriched for proteins associated with DNA replication and repair. These proteins include a small number of well-characterized S-phase DDR substrates. Substrates potentially inhibited by the DDR include Cdc25, the phosphatase involved in promoting mitotic entry, and Cdc18, the original establishment protein involved in promoting DNA replication. Substrates whose functions are likely to be activated include Rad52 and Sfr1, the recombinational-repair mediators, Rad2, the repair endonuclease, and Pfh1, the repair helicase. These results suggest that there are a large number of cytoskeletal- and cytokinesis-associated targets, each of which may make minor contributions to the S-phase DDR, but a smaller number of DNA replication and repair targets, each which is critical to surviving S-phase DNA damage. Consistent with this possibility, the Sty1 and Wis1 stress-induced MAP kinases are both required for MMS resistance but have no obvious targets that are required for MMS resistance, presumably because each target contributes only subtly to MMS resistance.

The S-phase DDR exists throughout eukaryotes, and the role of ATR as the central S-phase checkpoint kinase appears to be conserved (5). However, the effector kinases that regulate the S-phase DDR vary across evolution (8). Therefore, the extent to which the specific targets of the S-phase DDR would be conserved

has been unclear. Our data allow us to compare S-phase DDR targets in two distantly related yeasts, the fission yeast *S. pombe* and the budding yeast *Saccharomyces cerevisiae*, which are separated by about 300 My of evolution and have different arrangements of S-phase DDR effector kinases. Fission yeasts have Cds1 as a single effector kinase, an arrangement conserved across the fission yeast clade (55). Budding yeasts have two effector kinases: the downstream kinase Dun1, a Chk2 homolog with a canonical N-terminal FHA phosphopeptide-binding domain, such as Cds1, and the upstream kinase Rad53, a Chk2 homolog that has both N- and C-terminal FHA domains and which appears to phosphorylate many of the budding yeast S-phase DDR targets (14). These differences in effector kinases notwithstanding, the S-phase targets of the two species are highly conserved ($P < 10^{-10}$) (Fig. 5 and Dataset S1, Table S3).

The difference between the metazoan and fungal S-phase DDR pathways is even greater. Chk1 is the primary S-phase effector kinase in metazoans, whereas Chk2 fulfills that role in yeast (8). Nonetheless, we find significant conservation of S-phase DDR targets between fission yeasts and humans in the processes of chromatin regulation, transcription elongation, RNA processing, nuclear export, and DNA regulation. These results suggest that the general biological processes regulated by the S-phase DDR are important for a robust response to S-phase DNA damage and that the individual S-phase DDR targets are critical for regulating these processes properly.

Beyond the directly conserved targets, we find several broad categories of proteins that are targeted in both fission yeast and human cells (15, 47). In addition to the conserved cytoskeletal targets discussed above, both species target a variety of proteins involved in cytokinesis, suggesting that the DDR regulates not only the decision to divide but also the mechanics of cell division. Moreover, both species target gene expression at multiple levels, including transitional initiation, pre-mRNA splicing, and translation. These results suggest that the subtle regulation of cellular structure and gene expression plays an important and conserved role in the response to S-phase DNA damage and that, although none of these targets alone may have a profound effect on cell viability, the coordinated regulation of these cellular systems may be critical for genome stability over evolutionary time.

Materials and Methods

General Fission Yeast Methods. Cells were grown in YES (yeast extract plus supplements) medium at 30 °C using standard protocols (56). The following strains were used: yFS942 (h– leu1-32 ura4-D18 ade6-M210 his3-D1 cdc10-M17), AMC501 (h– leu1-32 ura4-D18 ade6-704), yFS943 (h– leu1-32 ura4-D18 ade6-M210 his3-D1 cdc10-M17 cds1::ura4), and yFS944 (h+ leu1-32 ura4-D18 cdc10-M17 rad3::ura4).

For S-phase MMS treatment, cells were synchronized by a combination of a Cdc10ts G1 arrest and release and centrifugal elutriation to select cells that were held for the least amount of time possible at the restrictive temperature (57, 58). For phosphopeptide-enriched MS, 300 OD units of cells were left untreated or were treated with 0.03% MMS from G1 and were harvested in mid-S phase, pelleted, and frozen in liquid nitrogen (Fig. S1). For anti-pSQ enrichment, between 3,000 and 4,000 OD units of cells were harvested from two or three cultures, using the same approach.

Because HU arrests cells in S phase and IR arrests cells in G2, we collected cells for our HU and IR datasets both from cultures presynchronized by elutriation and from cultures synchronized by treatment. For synchronous HU treatment, cells were synchronized in G2 by elutriation, treated with 10 mM HU, allowed to enter S phase, and harvested (Fig. S1). For asynchronous HU treatment, cells were treated with 10 mM HU for 165 min, at which time all cells in the culture had arrested in S phase, and were harvested. For synchronous IR treatment, cells were synchronized in G2 by elutriation, allowed to complete one full cell cycle and treated with 200 Gy in G2, allowed to recover for 20 min, and harvested (Fig. S1). For asynchronous IR treatment, asynchronous cells (80% of which were in G2) were treated with 200 Gy, allowed to recover for 20 min, and harvested. In each case, cells at 100–240 OD units were harvested for each sample, pelleted, and frozen in liquid nitrogen. All samples were prepared in duplicate and were pooled for analysis.

Reductive Dimethylation Labeling of Peptides. Cells were resuspended in 8 M urea lysis buffer and lysed by bead-beater disruption. Lysates were reduced with 4.5 mM DTT and alkylated with iodoacetamide. Proteins were digested with trypsin, and peptides were purified on C18 solid-phase extraction cartridges. Lyophilized peptides were labeled in vitro using reductive dimethyl labeling as previously described (59). For light cells (cells treated to induce DNA damage), peptides were dissolved in 1 M Hepes (pH 7.5) and were treated with 0.56 mL of 60 mM sodium cyanoborohydride and 0.56 mL of 4% formaldehyde for 20 min at room temperature. For heavy (untreated) cells, peptides in 1 M Hepes (pH 7.5) were treated with 0.56 mL of 60 mM (D3)-sodium cyanoborodeuteride and 0.56 mL of 4% deuterated (D2)-formaldehyde. Reactions were quenched with acetic acid, and dimethylated peptides were desalted using a Sep-Pak C18 cartridge (Waters). Light and heavy peptides were combined in a 1:1 ratio and lyophilized for further use.

Strong Cation Exchange Chromatography/Immobilized Metal Affinity Chromatography and Phospho-Antibody Immunoprecipitation Enrichment of Phosphopeptides. Strong cation exchange chromatography (SCX) and immobilized metal affinity chromatography (IMAC) were performed as previously described (47). Briefly, heavy and light labeled peptides were separated on a 9.4- × 200-mm column packed with polySULFOETHYL Aspartamide (The Nest Group Inc.). Twelve fractions were collected by salt gradient elution, desalted using 1 mL tC18 Sep-Pak cartridges (Waters), and lyophilized. One-half of each peptide solution was resuspended in 200 μL IMAC buffer (250 mM acetic acid, 30% acetonitrile) and enriched by 90-min incubation with 50 μL IMAC resin (PHOS-Select iron affinity gel; Sigma-Aldrich). The other half was resuspended in 200 μL of TiO2 buffer (2 M dihydroxybenzoic acid, 50% acetonitrile, 0.1% TFA) and enriched by 90-min incubation with 50 μL of Titansphere TiO2 beads (GL Sciences). Beads were washed with IMAC or TiO2 buffer, respectively, and were eluted with 50 mM Tris, 300 mM NH_4OH, pH 10.0. For phospho-antibody immunoprecipitation, peptides were dissolved in immunoprecipitation buffer [100 mM 3-(N-morpholino)propanesulfonic acid (pH 7.2), 10 mM sodium phosphate, 50 mM NaCl] and incubated with 50 μg anti-pSQ motif antibody (Cell Signaling Technology) immobilized on Protein A Sepharose beads. Beads were washed three times with immunoprecipitation buffer and twice with water. Bound phosphopeptides were eluted with 0.015% TFA, lyophilized, and desalted by stage-tip chromatography before LC-MS/MS.

MS and Quantification. Samples were analyzed in a hybrid Orbitrap XL mass spectrometer (Thermo Fisher). MS/MS spectra were searched using Sequest with the following parameters: three missed tryptic cleavages, and static modifications of 57.02146 Da (carboxyamidomethylation) on cysteine, 28.0313 (light dimethylation) on lysine, and 28.0313 (light dimethylation) on the peptide N terminus. Dynamic modifications included 79.96633 Da (phosphorylation) on serine, threonine, and tyrosine, 15.99491 Da (oxidation) on methionine, 6.03705 Da (heavy dimethylation) on lysine, and 6.03705 Da (heavy dimethylation) on the peptide N terminus. Matches were filtered to a false-discovery rate (FDR) of <1% by simultaneous searching of a reverse-sequence database and linear discriminant analysis. Automated peptide quantification was performed using the Vista program (24). Phosphopeptides were required to have a Vista confidence score greater than 80, and the sum of signal-to-noise values for the heavy and light peptides was required to be greater than 8.0. Sites with a more than twofold increase in light/heavy ratio were considered to be regulated.

Computational Analysis of Identified Phosphopeptides. Phosphopeptides in each dataset that were enriched more than twofold were selected for analysis, and partial digestion products were manually merged. Phosphorylation-site motif analysis was performed with Motif-X using the default setting and *S. pombe* proteome as background (33, 34). Logos were generated using pLogo with the *S. pombe* proteome as background (60). The significance of the abundance of specific phosphomotifs (RxxpS or pSQ) in our datasets was calculated with Fisher's exact test using peptides or proteins that were enriched more than and less than twofold as the groups and peptides or proteins that contained and did not contain the motif of interest as the categories. Gene-set enrichment was performed with custom Perl scripts using hypergeometric test-based enrichment analyses of genes in our datasets relative to the curated *S. pombe* GO categories (43). Only terms that had an FDR-corrected *P* value <0.05 were selected. Clustergrams were created with esyN using *S. pombe* using BioGRID and manually curated interactions (43, 61, 62).

ACKNOWLEDGMENTS. We thank Moran Yassour and Ilan Wapinski for the scripts used for gene set enrichment analysis and Yongjie Xu and members of the A.M.C., S.J.E., and N.R. laboratories for helpful discussions. This work was

supported by NIH Grants GM098815 (to N.R.) and GM44664 and AG011085 (to S.J.E.) and by Medical Research Council Grant G01100074 (to A.M.C.). A.E.H.E. is supported by a Burroughs Wellcome Fund CAMS award. S.J.E. is an Investigator with the Howard Hughes Medical Institute.

1. Kastan MB, Bartek J (2004) Cell-cycle checkpoints and cancer. *Nature* 432(7015):316–323.
2. Zhou BB, Elledge SJ (2000) The DNA damage response: Putting checkpoints in perspective. *Nature* 408(6811):433–439.
3. Branzei D, Foiani M (2009) The checkpoint response to replication stress. *DNA Repair (Amst)* 8(9):1038–1046.
4. Ciccia A, Elledge SJ (2010) The DNA damage response: Making it safe to play with knives. *Mol Cell* 40(2):179–204.
5. Sancar A, Lindsey-Boltz LA, Unsal-Kaçmaz K, Linn S (2004) Molecular mechanisms of mammalian DNA repair and the DNA damage checkpoints. *Annu Rev Biochem* 73:39–85.
6. Maréchal A, Zou L (2013) DNA damage sensing by the ATM and ATR kinases. *Cold Spring Harb Perspect Biol* 5(9):a012716.
7. Reinhardt HC, Yaffe MB (2009) Kinases that control the cell cycle in response to DNA damage: Chk1, Chk2, and MK2. *Curr Opin Cell Biol* 21(2):245–255.
8. Rhind N, Russell P (2000) Chk1 and Cds1: Linchpins of the DNA damage and replication checkpoint pathways. *J Cell Sci* 113(Pt 22):3889–3896.
9. Zou L, Elledge SJ (2003) Sensing DNA damage through ATRIP recognition of RPA-ssDNA complexes. *Science* 300(5625):1542–1548.
10. Liu Q, et al. (2000) Chk1 is an essential kinase that is regulated by Atr and required for the G(2)/M DNA damage checkpoint. *Genes Dev* 14(12):1448–1459.
11. Sanchez Y, et al. (1996) Regulation of RAD53 by the ATM-like kinases MEC1 and TEL1 in yeast cell cycle checkpoint pathways. *Science* 271(5247):357–360.
12. Rhind N, Russell P (1998) The Schizosaccharomyces pombe S-phase checkpoint differentiates between different types of DNA damage. *Genetics* 149(4):1729–1737.
13. Lindsay HD, et al. (1998) S-phase-specific activation of Cds1 kinase defines a subpathway of the checkpoint response in Schizosaccharomyces pombe. *Genes Dev* 12(3):382–395.
14. Liao H, Byeon IJ, Tsai MD (1999) Structure and function of a new phosphopeptide-binding domain containing the FHA2 of Rad53. *J Mol Biol* 294(4):1041–1049.
15. Matsuoka S, et al. (2007) ATM and ATR substrate analysis reveals extensive protein networks responsive to DNA damage. *Science* 316(5828):1160–1166.
16. Nakamura TM, Du LL, Redon C, Russell P (2004) Histone H2A phosphorylation controls Crb2 recruitment at DNA breaks, maintains checkpoint arrest, and influences DNA repair in fission yeast. *Mol Cell Biol* 24(14):6215–6230.
17. Zhao H, Tanaka K, Nogochi E, Nogochi C, Russell P (2003) Replication checkpoint protein Mrc1 is regulated by Rad3 and Tel1 in fission yeast. *Mol Cell Biol* 23(22):8395–8403.
18. Tanaka K, Boddy MN, Chen XB, McGowan CH, Russell P (2001) Threonine-11, phosphorylated by Rad3 and atm in vitro, is required for activation of fission yeast checkpoint kinase Cds1. *Mol Cell Biol* 21(10):3398–3404.
19. Lambert S, et al. (2003) Schizosaccharomyces pombe checkpoint response to DNA interstrand cross-links. *Mol Cell Biol* 23(13):4728–4737.
20. Boddy MN, Furnari B, Mondesert O, Russell P (1998) Replication checkpoint enforced by kinases Cds1 and Chk1. *Science* 280(5365):909–912.
21. Wilson-Grady JT, Villén J, Gygi SP (2008) Phosphoproteome analysis of fission yeast. *J Proteome Res* 7(3):1088–1097.
22. Tanaka K, Russell P (2001) Mrc1 channels the DNA replication arrest signal to checkpoint kinase Cds1. *Nat Cell Biol* 3(11):966–972.
23. Bentley NJ, et al. (1996) The *Schizosaccharomyces pombe rad3* checkpoint gene. *EMBO J* 15(23):6641–6651.
24. Bakalarski CE, et al. (2008) The impact of peptide abundance and dynamic range on stable-isotope-based quantitative proteomic analyses. *J Proteome Res* 7(11):4756–4765.
25. Brondello JM, Boddy MN, Furnari B, Russell P (1999) Basis for the checkpoint signal specificity that regulates Chk1 and Cds1 protein kinases. *Mol Cell Biol* 19(6):4262–4269.
26. Furnari B, Blasina A, Boddy MN, McGowan CH, Russell P (1999) Cdc25 inhibited in vivo and in vitro by checkpoint kinases Cds1 and Chk1. *Mol Biol Cell* 10(4):833–845.
27. O'Neill T, et al. (2002) Determination of substrate motifs for human Chk1 and hCds1/Chk2 by the oriented peptide library approach. *J Biol Chem* 277(18):16102–16115.
28. Rhind N, Russell P (1998) Tyrosine phosphorylation of cdc2 is required for the replication checkpoint in Schizosaccharomyces pombe. *Mol Cell Biol* 18(7):3782–3787.
29. Furnari B, Rhind N, Russell P (1997) Cdc25 mitotic inducer targeted by chk1 DNA damage checkpoint kinase. *Science* 277(5331):1495–1497.
30. Zeng Y, et al. (1998) Replication checkpoint requires phosphorylation of the phosphatase Cdc25 by Cds1 or Chk1. *Nature* 395(6701):507–510.
31. Ward IM, Chen J (2001) Histone H2AX is phosphorylated in an ATR-dependent manner in response to replicational stress. *J Biol Chem* 276(51):47759–47762.
32. Rozenzhak S, et al. (2010) Rad3 decorates critical chromosomal domains with gammaH2A to protect genome integrity during S-Phase in fission yeast. *PLoS Genet* 6(7):e1001032.
33. Chou MF, Schwartz D (2011) Biological sequence motif discovery using motif-x. *Curr Protoc Bioinformatics* Chapter 13:Unit 13.15–13.24.
34. Schwartz D, Gygi SP (2005) An iterative statistical approach to the identification of protein phosphorylation motifs from large-scale data sets. *Nat Biotechnol* 23(11):1391–1398.
35. Ashburner M, et al.; The Gene Ontology Consortium (2000) Gene ontology: Tool for the unification of biology. *Nat Genet* 25(1):25–29.
36. House NC, Koch MR, Freudenreich CH (2014) Chromatin modifications and DNA repair: Beyond double-strand breaks. *Front Genet* 5:296.
37. Dutta C, et al. (2008) The DNA replication checkpoint directly regulates MBF-dependent G1/S transcription. *Mol Cell Biol* 28(19):5977–5985.
38. de Bruin RA, et al. (2008) DNA replication checkpoint promotes G1-S transcription by inactivating the MBF repressor Nrm1. *Proc Natl Acad Sci USA* 105(32):11230–11235.
39. Gasch AP, et al. (2001) Genomic expression responses to DNA-damaging agents and the regulatory role of the yeast ATR homolog Mec1p. *Mol Biol Cell* 12(10):2987–3003.
40. Desany BA, Alcasabas AA, Bachant JB, Elledge SJ (1998) Recovery from DNA replicational stress is the essential function of the S-phase checkpoint pathway. *Genes Dev* 12(18):2956–2970.
41. Bastos de Oliveira FM, et al. (2015) Phosphoproteomics reveals distinct modes of Mec1/ATR signaling during DNA replication. *Mol Cell* 57(6):1124–1132.
42. Brown EJ, Baltimore D (2003) Essential and dispensable roles of ATR in cell cycle arrest and genome maintenance. *Genes Dev* 17(5):615–628.
43. Wood V, et al. (2012) PomBase: A comprehensive online resource for fission yeast. *Nucleic Acids Res* 40(Database issue):D695–D699.
44. Deshpande GP, et al. (2009) Screening a genome-wide S. pombe deletion library identifies novel genes and pathways involved in genome stability maintenance. *DNA Repair (Amst)* 8(5):672–679.
45. Zhou C, et al. (2016) Profiling DNA damage induced phosphorylation in budding yeast reveals diverse signaling networks. *Proc Natl Acad Sci USA* 113:E3667–E3675.
46. Smolka MB, Albuquerque CP, Chen SH, Zhou H (2007) Proteome-wide identification of in vivo targets of DNA damage checkpoint kinases. *Proc Natl Acad Sci USA* 104(25):10364–10369.
47. Elia AE, et al. (2015) Quantitative proteomic atlas of ubiquitination and acetylation in the DNA damage response. *Mol Cell* 59(5):867–881.
48. Kim ST, Lim DS, Canman CE, Kastan MB (1999) Substrate specificities and identification of putative substrates of ATM kinase family members. *J Biol Chem* 274(53):37538–37543.
49. Willis N, Rhind N (2009) Mus81, Rhp51(Rad51), and Rqh1 form an epistatic pathway required for the S-phase DNA damage checkpoint. *Mol Biol Cell* 20(3):819–833.
50. Amanchy R, et al. (2007) A curated compendium of phosphorylation motifs. *Nat Biotechnol* 25(3):285–286.
51. Chen D, et al. (2003) Global transcriptional responses of fission yeast to environmental stress. *Mol Biol Cell* 14(1):214–229.
52. Rosette C, Karin M (1996) Ultraviolet light and osmotic stress: Activation of the JNK cascade through multiple growth factor and cytokine receptors. *Science* 274(5290):1194–1197.
53. Devary Y, Rosette C, DiDonato JA, Karin M (1993) NF-kappa B activation by ultraviolet light not dependent on a nuclear signal. *Science* 261(5127):1442–1445.
54. Cortez D, Guntuku S, Qin J, Elledge SJ (2001) ATR and ATRIP: Partners in checkpoint signaling. *Science* 294(5547):1713–1716.
55. Rhind N, et al. (2011) Comparative functional genomics of the fission yeasts. *Science* 332(6032):930–936.
56. Forsburg SL, Rhind N (2006) Basic methods for fission yeast. *Yeast* 23(3):173–183.
57. Willis N, Rhind N (2011) Studying S-phase DNA damage checkpoints using the fission yeast Schizosaccharomyces pombe. *Methods Mol Biol* 782:13–21.
58. Willis N, Rhind N (2011) Studying G2 DNA damage checkpoints using the fission yeast Schizosaccharomyces pombe. *Methods Mol Biol* 782:1–12.
59. Hsu JL, Huang SY, Chow NH, Chen SH (2003) Stable-isotope dimethyl labeling for quantitative proteomics. *Anal Chem* 75(24):6843–6852.
60. O'Shea JP, et al. (2013) pLogo: A probabilistic approach to visualizing sequence motifs. *Nat Methods* 10(12):1211–1212.
61. Bean DM, et al. (2014) esyN: Network building, sharing and publishing. *PLoS One* 9(9):e106035.
62. Chatr-Aryamontri A, et al. (2015) The BioGRID interaction database: 2015 update. *Nucleic Acids Res* 43(Database issue):D470–D478.